

Single photons from dissipation in coupled cavities

H. Flayac and V. Savona

Institute of Theoretical Physics, École Polytechnique Fédérale de Lausanne EPFL, CH-1015 Lausanne, Switzerland

We propose a single photon source based on a pair of weakly nonlinear optical cavities subject to a one-directional dissipative coupling. When both cavities are driven by mutually coherent fields, sub-poissonian light is generated in the target cavity even when the nonlinear energy per photon is much smaller than the dissipation rate. The sub-poissonian character of the field holds over a delay measured by the inverse photon lifetime, as in the conventional photon blockade, thus allowing single-photon emission under pulsed excitation. We study a possible implementation of the dissipative coupling, compatible with current photonic platforms.

Introduction.— Single photon sources [1, 2] are a fundamental building block of most implementations of quantum information protocols. Current realizations based on the blockade mechanism [3] involve strong nonlinearities, with respect to the mode linewidths. They are usually engineered with such systems as quantum dots [4, 5], diamond color centers [6], superconducting circuits [7] or trapped atoms [8]. Although the degree of control over these systems is steadily improving, they basically operate at cryogenic temperatures and (or) imply significant fabrication challenges, particularly with respect to integration and scalability in future photonic platforms. On the other hand, nondeterministic sources relying on heralding protocols are now operating at room temperature in Silicon [9], but they require a significant input power for the the four wave mixing mechanism to set off [10, 11].

The Unconventional Photon Blockade [12] (UPB) was originally proposed as a mechanism to produce sub-poissonian light in presence of a very weak nonlinearity. The seminal system consists of a pair of coherently coupled cavities embedding a Kerr nonlinear medium, where one of the cavities is driven by a classical source [12–15]. It was then extended to Jaynes-Cummings [13], optomechanical [16] or bimodal cavity [17] systems and would be feasible in superconducting circuits [18]. It was shown that UPB essentially originates from a quantum interference mechanism [12, 13], that can arise even when the nonlinear energy per photon $U \ll \kappa$, where κ is the cavity photon loss rate.

UPB was shown to be within reach of an optimized silicon photonic crystal platform [19, 20], where it could lead to a new class of highly integrable, ultralow-power, passive single photon sources. However, the coherent mode coupling – with rate J – results a detrimental oscillation of the delayed second order correlation function $g^{(2)}(\tau)$, thus restricting the sub-Poissonian behaviour to photon delays shorter than $1/J \ll 1/\kappa$, i.e. much shorter than the photon lifetime under the required optimal antibunching conditions [13]. As a consequence, UPB is suppressed under pulsed excitation, as the sub-Poissonian portion of the time-dependent field contributes only minimally to the emitted pulse of duration $1/\kappa$ [20]. To

overcome this limitation, a strategy was recently proposed [20], where the output pulse is time-gated in order to retain only the sub-Poissonian contribution. An interesting alternative scheme, based on a weakly nonlinear three mode system, was also suggested in Ref.[21]. This scheme however requires a strong field driving one of the modes to effectively enhance the system nonlinearity, thus departing from the low-power operation that uniquely characterizes UPB.

The UPB can be understood in terms of Gaussian squeezed states, as clearly demonstrated in Ref.[22]. Indeed, for any coherent state $|\alpha\rangle$, there exists an optimal squeezing parameter ξ that minimizes the intensity fluctuations of the field to produce a nonclassical value of the two-photon correlation function, i.e. $g^{(2)}(0) < 1$. In a single mode Kerr resonator driven by a classical source [23, 24], the coherent and squeezing parameters α and ξ are linked to each other by the nature of the Kerr mechanism, in a way which departs from the optimal squeezing condition. The additional degrees of freedom of a two-mode system bring enough flexibility to tune the α and ξ parameters of the target mode independently. This leads to the strongly antibunched emission $g^{(2)}(0) \simeq 0$ at low driving field amplitude, $|\alpha| \rightarrow 0$. Within a simple picture, the auxiliary cavity acts as the source of squeezed light, while the driving field allows to tune the α parameter of the target cavity independently. The coherent, reversible coupling assumed in the original UPB scheme is therefore not a necessary condition. The main requirement is instead that of having an independently tunable squeezed light source.

With this idea at hand, in this Letter we demonstrate that the limitations of the UPB can be lifted by considering a cascaded cavity interaction [25–27] where the source cavity plays the role of a squeezed reservoir [28]. Indeed, as opposed to the case of a coherent interaction, in such system the nonlinearity and the cavity coupling magnitudes are essentially independent which allows to work with arbitrary laser-mode detunings. We find the optimal condition resulting in an almost perfect antibunching from potentially non-gaussian states, within the weak nonlinearity UPB paradigm. We then demonstrate the regularity of the $g^{(2)}(\tau)$ function, the pulsed operation

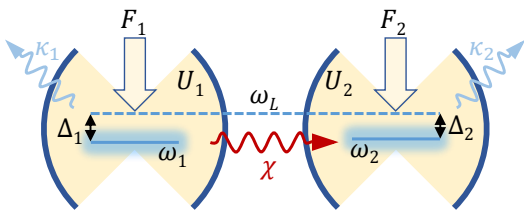


FIG. 1: (Color online) Scheme of the proposed system: Two nonlinear and dissipative optical resonators are driven by mutually coherent fields of same frequency ω_L but with different complex amplitudes $F_{1,2}$. The one-directional dissipative coupling from cavity 1 to cavity 2 occurs at a rate χ .

and propose a simple realization, relevant to current photonic systems [29], of the unidirectional coupling towards a flawless passive photon turnstile.

The Model.— We consider two single mode cavities with dissipative (one-directional) coupling from the first to the second cavity. We assume that both cavities embed a Kerr medium. The system is sketched in Fig.1. Our goal is to find a regime of parameters for which cavity 2 – from now on denoted target cavity – displays sub-poissonian photon statistics. The creation and annihilation operators of photons in each cavity are denoted by $\hat{a}_{1,2}^\dagger$ and $\hat{a}_{1,2}$. In the frame rotating at the frequency ω_L of the driving fields, the system Hamiltonian then reads

$$\hat{\mathcal{H}} = \sum_{j=1,2} \left[-\Delta_j \hat{a}_j^\dagger \hat{a}_j + U_j \hat{a}_j^\dagger \hat{a}_j^\dagger \hat{a}_j \hat{a}_j + F_j^* \hat{a}_j + F_j \hat{a}_j^\dagger \right], \quad (1)$$

where F_j ($j = 1, 2$) are the driving field amplitudes for each cavity, $\Delta_j = \omega_j - \omega_L$ are the cavity mode detunings, and U_j are the strengths of the Kerr nonlinearities. The open system dynamics obeys the quantum master equation for its density matrix $\hat{\rho}$

$$i \frac{\partial \hat{\rho}}{\partial t} = \left[\hat{\mathcal{H}}, \hat{\rho} \right] - \frac{i}{2} \sum_{j=1,2} \kappa_j \hat{\mathcal{D}}[\hat{a}_j] \hat{\rho} + i\chi \hat{\mathcal{D}}[\hat{a}_1, \hat{a}_2] \hat{\rho}, \quad (2)$$

where $\hat{\mathcal{D}}[\hat{a}_j] \hat{\rho} = \{\hat{a}_j^\dagger \hat{a}_j, \hat{\rho}\} - 2\hat{a}_j \hat{\rho} \hat{a}_j^\dagger$ describe the dissipation of each cavity into the environment at rates κ_j , and $\hat{\mathcal{D}}[\hat{a}_1, \hat{a}_2] \hat{\rho} = [\hat{a}_1 \hat{\rho}, \hat{a}_2^\dagger] + [\hat{a}_2, \hat{\rho} \hat{a}_1^\dagger]$ models the dissipative coupling from cavity 1 to cavity 2 at a rate $\chi = \sqrt{\eta \kappa_1 \kappa_2}$. Here, we have defined a transfer efficiency $\eta \in [0, 1]$ [30], relating the coupling to the dissipation rates.

Before solving Eq. (44) for the stationary state, it is useful to study the system in the weak pump limit $F_{1,2} \rightarrow 0$. In this limit, analytical expressions for the various expectation values can be obtained by restricting to the $n \leq 2$ photon manifold [13, 15, 16]. Details of this analysis are reported in the Supplemental Material [31]. In this limit, the two photon correlations of the target

cavity approximates to

$$g_2^{(2)}(0) = \frac{\langle \hat{a}_2^\dagger \hat{a}_2^\dagger \hat{a}_2 \hat{a}_2 \rangle}{\langle \hat{a}_2^\dagger \hat{a}_2 \rangle^2} \simeq 2 \frac{|c_{02}|^2}{|c_{01}|^4} \quad (3)$$

where $|c_{01}|^2$ and $|c_{02}|^2$ are the probabilities of having zero photons in cavity 1 and, respectively, 1 and 2 photons in the target cavity. By requiring $c_{02} = 0$, one obtains a condition for optimal sub-poissonian behaviour, $g_2^{(2)}(0) \simeq 0$, in this limit. We find that this optimal condition can be met for all values of the intrinsic system parameters, provided the driving field amplitudes fulfill the relation

$$F_1|_{\text{opt}} = iF_2 \frac{\tilde{\Delta} \tilde{U}_1 \pm \sqrt{-U_1 \tilde{U}_1 \tilde{\Delta} \tilde{\Delta}_2}}{(\tilde{\Delta} + U_1) \chi}, \quad (4)$$

where $\tilde{\Delta}_{1,2} = -\Delta_{1,2} - i\kappa_{1,2}/2$, $\tilde{\Delta} = \tilde{\Delta}_1 + \tilde{\Delta}_2$, $\tilde{U}_1 = \tilde{\Delta}_1 + U_1$, and assuming $F_2 \in \mathbb{R}$ without loss of generality. Eq.(22) reveals several interesting features: (i) $F_1|_{\text{opt}}$ is complex-valued, so it needs to carry an optimal phase in addition to the proper magnitude. (ii) $F_1|_{\text{opt}}$ depends linearly on F_2 , which cannot therefore be set to zero. This can be qualitatively understood from the fact that, if the target cavity is not driven, then it simply acts as a spectral filter for the field originating from cavity 1 [32], thus essentially recovering the single cavity emission statistics. (iii) The optimal field amplitude doesn't depend on U_2 , which can therefore be set arbitrarily small. If under the assumption that the sub-poissonian character originates from the optimal squeezing mechanism described in Ref.[22], then this feature hints at the fact that cavity 1 is here the main source of squeezing. (iv) In the case where $U_1 = 0$, an optimal value of the driving field is still well defined but results in a vanishing occupation of the target cavity. (v) We made no assumption so far on the value of U_1 , which may be therefore set arbitrarily smaller or larger than the loss rates κ_j .

Results and Discussion.— From now on, we will consider the case of cavities with equal loss rates $\kappa_1 = \kappa_2 = \kappa$ and nonlinearities $U_1 = U_2 = U$. We numerically solve Eq. (44) in the stationary limit, on a Hilbert space truncated to include N_{max} quanta per mode against which the convergence of the results was carefully checked. As a figure of merit, in Fig.2(a), we have plotted (blue line) the equal-time two-photon correlation $g_2^{(2)}(0)$ for the target cavity, as a function of its average occupation n_2 . The pairs of values were obtained by increasing F_2 and keeping $F_1 = F_1|_{\text{opt}}$, with the nonlinearity set to $U/\kappa = 10^{-3}$. For this calculation we additionally assumed $\chi = \kappa$ and $\Delta_1 = \Delta_2 = 0$ for simplicity.

Computing the exact numerical solution for increasing driving field amplitudes becomes cumbersome, as the value of N_{max} required for convergence becomes exceedingly large. As an alternative, we have solved the corresponding model linearized with respect to the mean-field

solution (as detailed in the Supplemental Material [31]). The result is plotted as a red line in Fig. 2(a) and significantly extends the range of accessible n_2 values. We notice that the linearized model doesn't hold in the limit of very small occupancies, where quantum fluctuations dominate over the mean-field. The optimal two-photon correlation behaves linearly as a function of n_2 , with the exception of large occupancy where a nonlinear increase of $g_2^{(2)}(0)$ is displayed in the red curve. The reason of this behaviour resides in the limited range of validity of Eq. (22) which assumes small occupancies. For larger values of n_2 we therefore searched for the optimal parameters numerically, by applying a genetic optimization procedure to the linearized model and using the modulus and phase of F_1 as free parameters. The result is displayed in Fig. 2(a) as a yellow line. The value $g_2^{(2)} \leq 0.5$ – here considered as an upper bound for single-photon emission – is reached for a remarkably high occupancy $n_2 \simeq 0.25$.

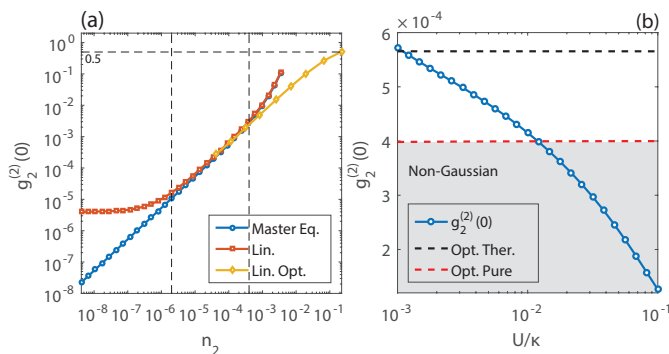


FIG. 2: (Color online) (a) Two-photon correlation $g_2^{(2)}(0)$ in the target cavity as a function of its occupation n_2 in the case where $U = 10^{-3}\kappa$ and $F_1 = F_1|_{\text{opt}}$ from Eq. (22). Blue line: exact master equation. Red line: linearized model. Yellow line: linearized model where F_1 was obtained for each value of n_2 from numerical minimization of $g_2^{(2)}(0)$. (b) Two-photon correlation $g_2^{(2)}(0)$ versus the nonlinear energy U at fixed occupation $n_2 = 10^{-4}$. The dashed black and red line denote the thermal and pure state boundaries set for a Gaussian state in Ref. 22.

Under the assumption that the state is Gaussian, it was shown [22] that a lower bound on $g^{(2)}(0)$ exists. In particular, for $n \ll 1$, this lower bound is given by $g^{(2)}(0)|_{\text{p}} \simeq 4|\langle \hat{a} \rangle|^2$ for a pure displaced-squeezed state, and by $g^{(2)}(0)|_{\text{th}} = 8\sqrt{\bar{n}_{\text{eff}}}$ for a corresponding thermal (i.e. mixed) state with thermal occupation \bar{n}_{eff} . For a more general mixed state, we can define an effective thermal occupation $\bar{n}_{\text{eff}} = (1/\text{Tr}\hat{\rho}^2 - 1)/2 \ll 1$, which then roughly measures the degree of mixedness of the state. We have therefore computed in Fig.2(b) $g_2^{(2)}(0)$ versus U (blue line) at a fixed occupation $n_2 = 10^{-4}$ compared both to the pure and thermal limits (dashed lines) that are obviously constant for given n_2 and κ values. Photons in the target cavity clearly achieve a value of $g^{(2)}(0)$

lying below the thermal limit and, for $U/\kappa > 10^{-2}$, lying even below the limit set for pure Gaussian state. In this latter case, we have checked (not shown) that the state departs from a Gaussian state, with the Wigner distribution taking negative values. Obviously, the non Gaussian feature is not present in the result obtained for the same parameters from the linearized model.

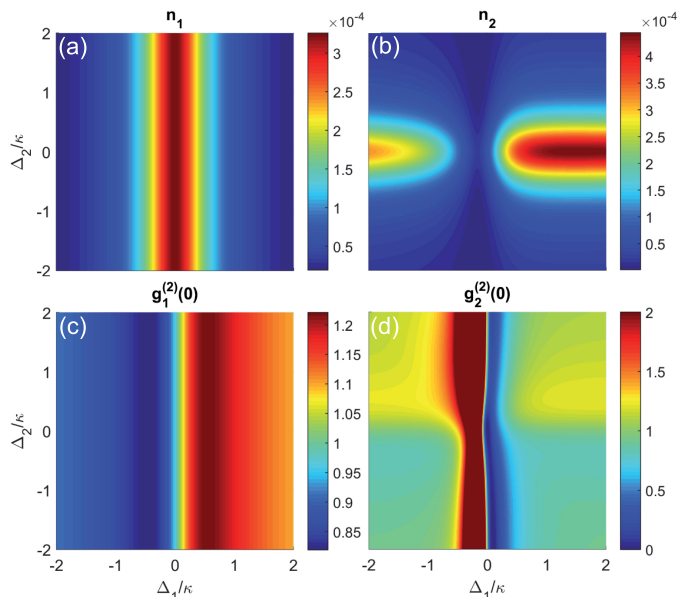


FIG. 3: (Color online) Color maps of (a)-(b) the cavity occupation $n_{1,2}$ and (c)-(d) the two-photon correlation function $g_{1,2}^{(2)}(0)$, computed as a function of the cavity detunings. Here $U = 10^{-3}\kappa$ and we set the optimal condition (22) at $\Delta_{1,2} = 0$ and $n_2 = 10^{-4}$.

We have studied the impact of variable detunings $\Delta_{1,2}$ when the other parameters are fixed. The results presented in Fig.2 where the panels (a) and (b) show the cavity occupations and the panels (c) and (d) the corresponding second order correlation function. Due to the dissipative nature of the coupling, cavity 1 behaves similarly to an isolated Kerr oscillator, with the field amplitude simply given by $\alpha_1 \simeq F_1/\tilde{\Delta}_1$. As one can see from Fig.2(c) the second order correlation function, which in this limit is given by $g_1^{(2)}(0) \approx |\tilde{\Delta}_1|^2/|\tilde{\Delta}_1 + U|^2$ [31], reveals a weak (anti)bunching at (negative) positive detunings. This is a signature of the (amplitude) phase squeezing induced by the Kerr nonlinearity [23, 24]. Therefore, cavity 1 acts as a weakly squeezed source that can be tuned by adjusting the laser frequency. The behaviour of the target cavity is less trivial. Counterintuitively, Fig.2(c) shows that the occupation vanishes for vanishing detuning. This is due to destructive interference between the input from cavity 1 and the field driving the target cavity. In particular one obtains $n_2 = 0$ under the condition $F_2 = -i\chi F_1/\tilde{\Delta}_1$ [31]. In this region, we observe both a strong bunching up to $g_2^{(2)}(0) = 30$ (red areas) or

strong antibunching (blue areas) where the optimal $g_2^{(0)}$ conditions hold. Such nonclassical statistics results from the interplay between the squeezing brought by cavity 1 and the field displacement induced by the driving field on the target cavity [22]. We note that the results remain almost unchanged when $U_2 = 0$ (not shown) as prescribed by Eq.(22).

As discussed above, the UPB scheme displays antibunching only for values of the time delay smaller than $1/J \ll 1/\kappa$ [12, 13, 20], thus preventing simple operation under pulsed input. The present scheme overcomes this difficulty. We show in Fig.4 the computed $g_2^{(2)}(\tau)$ for the optimal parameter values (red line) compared to the UPB behavior (blue line) for the same value of U (see captions). Remarkably, in the dissipative case, the antibunching survives over a time scale of about $\tau = 10/\kappa$ and oscillations are absent due to the fact that the optimal antibunching occurs here at zero detuning. The single photon regime, defined by $g_2^{(2)}(\tau) < 0.5$, is preserved on a time scale as large as $\tau = 5/\kappa$ (gray area) and behaves similarly to conventional sources [3].

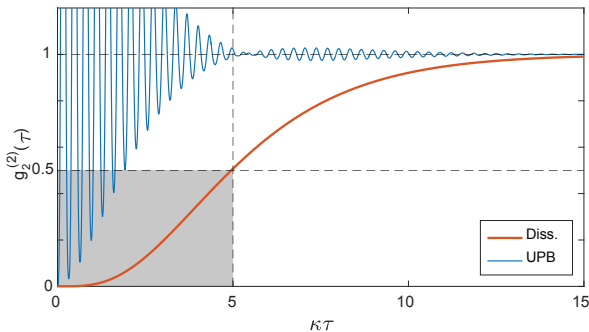


FIG. 4: (Color online) Delayed two-photon correlation function $g_2^{(2)}(\tau)$ (red line) computed for the target cavity at $n_2 = 10^{-4}$ and $U = 10^{-3}\kappa$. The gray area highlights the single photon regime. The blue line shows the oscillating UPB counterpart obtained for the same values of U requiring $J = 19.6\kappa$, $\Delta_j = 0.29\kappa$ and $F_1 = 0$.

Pulsed Regime.— We study the pulsed regime in more detail by a direct time integration of Eq.(44). We assume input Gaussian pulses $F_j \exp[-(t - t_{j0})^2/\sigma_t^2]$. A key quantity in assessing the single-photon emission under pulsed excitation is the two-photon correlation averaged over the two times, defined as [20]

$$g_{\text{pulse}}^{(2)} = \frac{\int G_2^{(2)}(t_1, t_2) dt_1 dt_2}{\int n_2(t_1) n_2(t_2) dt_1 dt_2} \quad (5)$$

where $G_2^{(2)}(t_1, t_2) = \langle \hat{a}_2^\dagger(t_1) \hat{a}_2^\dagger(t_2) \hat{a}_2(t_2) \hat{a}_2(t_1) \rangle$ and $n_2(t) = \langle \hat{a}_2^\dagger(t) \hat{a}_2(t) \rangle$. For an optimal single-photon operation, the excitation pulses must be optimized according to the following criteria: (i) The pulse duration should be shorter than the subpoissonian time window (see Fig.4),

while (ii) it should be long enough to allow the optimal condition relating the 2 cavity fields to dynamically set up. This latter condition occurs over a time inversely dependent on U . Moreover, if the pulses are simultaneous, the target cavity displays a pronounced bunching in the early emission, as can be also inferred from Fig.3(d). This effect can be overcome by introducing a suitable time delay $\Delta t = t_{02} - t_{01} = 1.5/\kappa$ between the two pulses [31].

We show in Fig.5(a) the computed cavity occupations $n_j(t)$. Here, the target cavity has an average occupation of $n_{\text{pulse}} = \int n_2(t) dt \simeq 3 \times 10^{-2}$. Fig. 5(b) shows the corresponding two-time second order coherence function $g_2^{(2)}(t_1, t_2)$. The overlay contour plot highlights the two-time occupation of the target cavity $n_2(t_1, t_2) = \sqrt{n_2(t_1)n_2(t_2)}$, which peaks well inside the sub-poissonian portion of the plot. For the present case, we obtain $g_{\text{pulse}}^{(2)} \simeq 0.3$. Single photon operation may be enhanced via an optimal pulse shaping (a task lying beyond the scope of this study). Further enhancement may be obtained through time-gating the output pulse, as already suggested for the UPB [20]. If we apply a time gate of duration $\Delta T = 5/\kappa$, highlighted by the dashed lines in Fig. 5(b), the two-photon correlation is reduced to $g_{\text{pulse}}^{(2)} < 0.1$ while preserving an average occupation of $n_{\text{pulse}} \simeq 10^{-2}$.

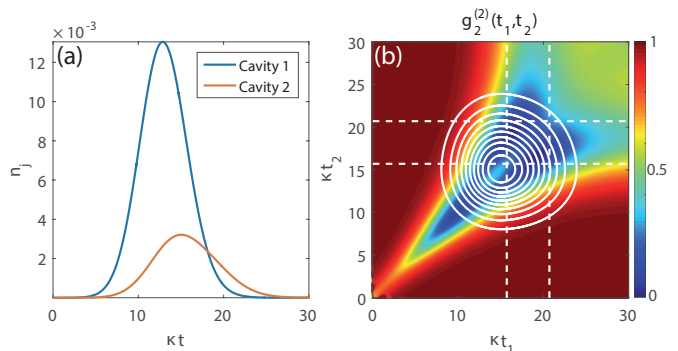


FIG. 5: (Color online) Pulsed regime: (a) Time dependent cavity occupation. (b) Two-time two-photon correlation function $g_2^{(2)}(t_1, t_2)$. The quantity $n_2(t_1, t_2)$ is displayed as a contour plot. The dashed-white lines denote a time-gate window resulting in $g_{\text{pulse}}^{(2)} < 0.1$. The parameters are here $U = 10^{-1}\kappa$, $\sigma_t = 5/\kappa$, $\Delta_j = 0$, $F_2 = 0.1\kappa$, $F_1 = F_1|_{\text{opt}}$ and the delay between the two excitation pulses is set to $\Delta = 1.5/\kappa$.

Realistic Implementation.— The dissipative coupling assumed in the present work can be implemented through an intermediate coupling element, which may be a waveguide or a third optical resonator, as investigated in Ref.[29]. In the latter case, the extra mode acts as an engineered reservoir, effectively generating the quantum interference required for the one-directional coupling. The

corresponding model Hamiltonian reads

$$\hat{H} = \sum_{j=1}^3 \left[-\Delta_j \hat{a}_j^\dagger \hat{a}_j + U_j \hat{a}_j^\dagger \hat{a}_j^\dagger \hat{a}_j \hat{a}_j + F_j^* \hat{a}_j + F_j \hat{a}_j^\dagger \right] + \sum_{j \neq k=1}^3 \left[J_{jk} \hat{a}_j^\dagger \hat{a}_k + J_{jk}^* \hat{a}_k^\dagger \hat{a}_j \right] \quad (6)$$

where the auxiliary mode is not driven, i.e. $F_3 = 0$, and is ideally characterized by a large dissipation rate $\kappa_3 \gg \kappa_{1,2}$. Here J_{jk} describe coherent photon hopping amplitudes. This system is well approximated by the dissipative coupling Eq. (44) under the conditions $J_{12} = i\chi/2$ and $J_{23} = J_{31} = \sqrt{-iJ_{12}\kappa_3}/2$. It requires a complex-valued J_{12} , currently feasible e.g. using waveguide delay lines as proposed in Ref.[33]. The one-directional operation can be tested by simulating the system in the situation where only the target cavity is driven. As shown in the Supplemental Material, a vanishing field is transmitted to cavity 1 [31] in that case. In presence of the auxiliary resonator, the optimal antibunching condition turn out to be displaced in the parameter space. We have identified the new optimal condition by running an automated optimization (in the steady state regime) with $|F_1|$ and ϕ_1 as free parameters, and setting $F_2 = 0.1\kappa$, $U_j = 10^{-3}\kappa$, $\Delta_j = 0$, and $\kappa_3 = 10\kappa$. We obtained a value of $g_2^{(2)}(0) = 3.8 \times 10^{-2}$ for $|F_1| = 6.58 \times 10^{-2}\kappa$ and $\phi_1 \simeq 0$, proving that the three-cavity implementation of the scheme can indeed display single-photon operation.

Conclusion.— We have proposed a scheme for a single-photon source operating under weak nonlinearity and relying on dissipative, one-directional coupling between two optical cavities. The dissipative coupling approach enables single-photon generation over pulsed excitation, thus overcoming the main limitation of the unconventional photon blockade. Although the main mechanism at the origin of antibunching is the optimal squeezing described by Lemonde *et al.* [22], the present scheme achieves a two-photon correlation lower than the lower bound expected for Gaussian states. We have proposed a three-cavity configuration that enables the one-directional coupling and may be realized on several platforms, including coupled ring resonators or photonic crystal cavities. The scheme could be generalized to several cascaded optical cavities, aiming at suppressing the n -photon probabilities to further enhance the single-photon operation.

Acknowledgments.— The authors acknowledge fruitful discussions with D. Gerace and M. Minkov.

[1] B. Lounis and M. Orrit, Reports on Progress in Physics **68**, 1129 (2005), ISSN 0034-4885, URL <http://stacks.iop.org/0034-4885/68/i=5/a=R04>.

- [2] M. D. Eisaman, J. Fan, A. Migdall, and S. V. Polyakov, Review of Scientific Instruments **82**, 071101 (2011), URL <http://scitation.aip.org/content/aip/journal/rsi/82/7/10.1063/1.3610677>.
- [3] H. Paul, Reviews of Modern Physics **54**, 1061 (1982), URL <http://link.aps.org/doi/10.1103/RevModPhys.54.1061>.
- [4] P. Michler, A. Kiraz, C. Becher, W. V. Schoenfeld, P. M. Petroff, L. Zhang, E. Hu, and A. Imamoglu, Science **290**, 2282 (2000), ISSN 0036-8075, 1095-9203, URL <http://www.sciencemag.org/content/290/5500/2282>.
- [5] C. Santori, M. Pelton, G. Solomon, Y. Dale, and Y. Yamamoto, Physical Review Letters **86**, 1502 (2001), URL <http://link.aps.org/doi/10.1103/PhysRevLett.86.1502>.
- [6] C. Kurtsiefer, S. Mayer, P. Zarda, and H. Weinfurter, Physical Review Letters **85**, 290 (2000), URL <http://link.aps.org/doi/10.1103/PhysRevLett.85.290>.
- [7] C. Lang, D. Bozyigit, C. Eichler, L. Steffen, J. M. Fink, A. A. Abdumalikov, M. Baur, S. Filipp, M. P. da Silva, A. Blais, et al., Physical Review Letters **106**, 243601 (2011), URL <http://link.aps.org/doi/10.1103/PhysRevLett.106.243601>.
- [8] J. McKeever, A. Boca, A. D. Boozer, R. Miller, J. R. Buck, A. Kuzmich, and H. J. Kimble, Science **303**, 1992 (2004), ISSN 0036-8075, 1095-9203, URL <http://www.sciencemag.org/content/303/5666/1992>.
- [9] M. Davano, J. R. Ong, A. B. Shehata, A. Tosi, I. Agha, S. Assefa, F. Xia, W. M. J. Green, S. Mookherjee, and K. Srinivasan, Applied Physics Letters **100**, 261104 (2012), ISSN 0003-6951, 1077-3118, URL <http://scitation.aip.org/content/aip/journal/apl/100/26/10.1063/1.4711253>.
- [10] J. Li, L. O’Faolain, I. H. Rey, and T. F. Krauss, Optics Express **19**, 4458 (2011), ISSN 1094-4087, URL <https://www.osapublishing.org/oe/abstract.cfm?uri=oe-19-5-4458>.
- [11] J. B. Spring, P. S. Salter, B. J. Metcalf, P. C. Humphreys, M. Moore, N. Thomas-Peter, M. Barbieri, X.-M. Jin, N. K. Langford, W. S. Kolthammer, et al., Optics Express **21**, 13522 (2013), ISSN 1094-4087, URL <https://www.osapublishing.org/oe/abstract.cfm?uri=oe-21-11-13522>.
- [12] T. C. H. Liew and V. Savona, Phys. Rev. Lett. **104**, 183601 (2010), URL <http://link.aps.org/doi/10.1103/PhysRevLett.104.183601>.
- [13] M. Bamba, A. Imamoglu, I. Carusotto, and C. Ciuti, Phys. Rev. A **83**, 021802 (2011), URL <http://link.aps.org/doi/10.1103/PhysRevA.83.021802>.
- [14] M. Bamba and C. Ciuti, Applied Physics Letters **99**, 171111 (pages 3) (2011), URL <http://link.aip.org/link/?APL/99/171111/1>.
- [15] H. Flayac and V. Savona, Physical Review A **88**, 033836 (2013), URL <http://link.aps.org/doi/10.1103/PhysRevA.88.033836>.
- [16] V. Savona, arXiv (2013), 1302.5937.
- [17] A. Majumdar, M. Bajcsy, A. Rundquist, and J. Vuckovic, Physical Review Letters **108**, 183601 (2012), URL <http://link.aps.org/doi/10.1103/PhysRevLett.108.183601>.
- [18] C. Eichler, Y. Salathe, J. Mlynek, S. Schmidt, and A. Wallraff, Physical Review Letters **113**, 110502 (2014), URL <http://link.aps.org/doi/10.1103/PhysRevLett.113.110502>.

- [19] S. Ferretti, V. Savona, and D. Gerace, *New Journal of Physics* **15**, 025012 (2013), URL <http://stacks.iop.org/1367-2630/15/i=2/a=025012>.
- [20] H. Flayac, D. Gerace, and V. Savona, *Scientific Reports* **5**, 11223 (2015), ISSN 2045-2322, URL <http://www.nature.com/doi/10.1038/srep11223>.
- [21] O. Kyriienko and T. C. H. Liew, *Physical Review A* **90**, 063805 (2014), URL <http://link.aps.org/doi/10.1103/PhysRevA.90.063805>.
- [22] M.-A. Lemonde, N. Didier, and A. A. Clerk, *Physical Review A* **90**, 063824 (2014), URL <http://link.aps.org/doi/10.1103/PhysRevA.90.063824>.
- [23] C. C. Gerry and R. Grobe, *Physical Review A* **49**, 2033 (1994), URL <http://link.aps.org/doi/10.1103/PhysRevA.49.2033>.
- [24] J. Bajer, A. Miranowicz, and R. Tana, *Czechoslovak Journal of Physics* **52**, 1313 (2002), ISSN 0011-4626, 1572-9486, URL <http://link.springer.com/article/10.1023/A%3A1021867510898>.
- [25] H. J. Carmichael, *Physical Review Letters* **70**, 2273 (1993), URL <http://link.aps.org/doi/10.1103/PhysRevLett.70.2273>.
- [26] C. W. Gardiner, *Physical Review Letters* **70**, 2269 (1993), URL <http://link.aps.org/doi/10.1103/PhysRevLett.70.2269>.
- [27] C. W. Gardiner and A. S. Parkins, *Physical Review A* **50**, 1792 (1994), URL <http://link.aps.org/doi/10.1103/PhysRevA.50.1792>.
- [28] N. Didier, F. Qassemi, and A. Blais, *Physical Review A* **89**, 013820 (2014), URL <http://link.aps.org/doi/10.1103/PhysRevA.89.013820>.
- [29] A. Metelmann and A. Clerk, *Physical Review X* **5**, 021025 (2015), URL <http://link.aps.org/doi/10.1103/PhysRevX.5.021025>.
- [30] C. Gardiner and P. Zoller, *Quantum Noise: A Handbook of Markovian and Non-Markovian Quantum Stochastic Methods with Applications to Quantum Optics* (Springer, 2004), ISBN 9783540223016.
- [31] *See supplemental material at [url] for more details.*
- [32] H. Flayac and V. Savona, *Physical Review Letters* **113**, 143603 (2014), URL <http://link.aps.org/doi/10.1103/PhysRevLett.113.143603>.
- [33] M. Hafezi, E. A. Demler, M. D. Lukin, and J. M. Taylor, *Nature Physics* **7**, 907 (2011), ISSN 1745-2473, URL <http://www.nature.com/nphys/journal/v7/n11/full/nphys2063.html>.

Supplemental Material

We provide useful analytical expressions of the system wavefunction in the limit of weak cavity driving, develop linearized and semiclassical approaches for large driving and demonstrate the efficient unidirectional transmission of the three cavities configuration.

WEAK PUMP LIMIT

Given the system Hamiltonian

$$\hat{\mathcal{H}} = \sum_{j=1,2} \left[-\Delta_j \hat{a}_j^\dagger \hat{a}_j + U_j \hat{a}_j^\dagger \hat{a}_j^\dagger \hat{a}_j \hat{a}_j + F_j^* \hat{a}_j + F_j \hat{a}_j^\dagger \right], \quad (1)$$

in the limit of weak driving fields $F_{1,2} \rightarrow 0$ and therefore low cavity occupations $n_{1,2} \rightarrow 0$, we can restrain the system wavefunction to the two-photons manifold

$$|\psi\rangle \simeq c_{00} |00\rangle + c_{10} |10\rangle + c_{01} |01\rangle + c_{11} |11\rangle + c_{20} |20\rangle + c_{02} |02\rangle \quad (2)$$

Here, $|jk\rangle$ denotes a Fock state with j photons in the first cavity and k photons in the second one. The wavefunction dynamics is found from the solution of the nonlinear Schrödinger equation $\tilde{\mathcal{H}}|\psi\rangle = i\hbar\partial_t|\psi\rangle$ written for the non-Hermitian Hamiltonian

$$\tilde{\mathcal{H}} = \hat{\mathcal{H}} - \frac{i}{2} \sum_{j=1,2} \kappa_j \hat{a}_j^\dagger \hat{a}_j - i\chi \hat{a}_1 \hat{a}_2^\dagger \quad (3)$$

where the first term stands for the cavities losses and the second one for the unidirectional transmission. We obtain the following coupled set of equations for the coefficients $c_{jk}(t)$

$$i\dot{c}_{00} = F_1 c_{10} + F_2 c_{01} \quad (4)$$

$$i\dot{c}_{10} = F_1 c_{00} + \tilde{\Delta}_1 c_{10} \quad (5)$$

$$i\dot{c}_{01} = F_2 c_{00} + \tilde{\Delta}_2 c_{01} - i\chi c_{10} \quad (6)$$

$$0 = F_1 \sqrt{2} c_{11} + F_2 c_{20} \quad (7)$$

$$0 = F_2 \sqrt{2} c_{11} + F_1 c_{02} \quad (8)$$

$$i\dot{c}_{20} = F_1 \sqrt{2} c_{10} + 2 \left(U_1 + \tilde{\Delta}_1 \right) c_{20} \quad (9)$$

$$i\dot{c}_{02} = F_2 \sqrt{2} c_{01} + 2 \left(U_2 + \tilde{\Delta}_2 \right) c_{02} - i\chi \sqrt{2} c_{11} \quad (10)$$

$$i\dot{c}_{11} = F_1 c_{01} + F_2 c_{10} + \left(\tilde{\Delta}_1 + \tilde{\Delta}_2 \right) c_{11} - i\chi \sqrt{2} c_{20} \quad (11)$$

In the steady state where $\dot{c}_{jk}(t) = 0$, imposing the normalization condition $c_{00} = 1$ and solving the resulting equations for the c_{jk} coefficients iteratively, we obtain

the explicit expressions

$$c_{10} = -\frac{F_1}{\tilde{\Delta}_1} \quad (12)$$

$$c_{01} = -\frac{F_2}{\tilde{\Delta}_2} - i\chi \frac{F_1}{\tilde{\Delta}_1 \tilde{\Delta}_2} \quad (13)$$

$$c_{11} = \frac{F_1 F_2}{\tilde{\Delta}_1 \tilde{\Delta}_2} + \frac{iF_1^2 \left(\tilde{\Delta}_1 + \tilde{\Delta}_2 + U_1 \right) \chi}{\tilde{\Delta}_1 \tilde{\Delta}_2 \left(\tilde{\Delta}_1 + \tilde{\Delta}_2 \right) \left(\tilde{\Delta}_1 + U_1 \right)} \quad (14)$$

$$c_{20} = \frac{F_1^2}{\tilde{\Delta}_1 \left(\tilde{\Delta}_1 + U_1 \right) \sqrt{2}} \quad (15)$$

$$c_{02} = \frac{F_2^2}{\tilde{\Delta}_2 \left(\tilde{\Delta}_2 + U_2 \right) \sqrt{2}} \quad (16)$$

$$+ \frac{2iF_1 F_2 \sqrt{2} \left(\tilde{\Delta}_1 + \tilde{\Delta}_2 \right) \left(\tilde{\Delta}_1 + U_1 \right) \chi}{\tilde{\Delta}_1 \tilde{\Delta}_2 \left(\tilde{\Delta}_1 + \tilde{\Delta}_2 \right) \left(\tilde{\Delta}_1 + U_1 \right) \left(\tilde{\Delta}_2 + U_2 \right)} - \frac{F_1^2 \left(\tilde{\Delta}_1 + \tilde{\Delta}_2 + U_1 \right) \chi^2}{\tilde{\Delta}_1 \tilde{\Delta}_2 \left(\tilde{\Delta}_1 + \tilde{\Delta}_2 \right) \left(\tilde{\Delta}_1 + U_1 \right) \left(\tilde{\Delta}_2 + U_2 \right)}$$

with the definition $\tilde{\Delta}_j = -\Delta_j - i\kappa_j/2$. The cavity occupations and second order coherence functions are then computed as

$$n_1 = \langle \hat{a}_1^\dagger \hat{a}_1 \rangle = |c_{10}|^2 + |c_{11}|^2 + 2|c_{20}|^2 \quad (17)$$

$$n_2 = \langle \hat{a}_2^\dagger \hat{a}_2 \rangle = |c_{01}|^2 + |c_{11}|^2 + 2|c_{02}|^2 \quad (18)$$

$$g_1^{(2)}(0) = \frac{\langle \hat{a}_1^\dagger \hat{a}_1^\dagger \hat{a}_1 \hat{a}_1 \rangle}{n_1^2} \simeq 2 \frac{|c_{20}|^2}{|c_{10}|^4} \quad (19)$$

$$g_2^{(2)}(0) = \frac{\langle \hat{a}_2^\dagger \hat{a}_2^\dagger \hat{a}_2 \hat{a}_2 \rangle}{n_2^2} \simeq 2 \frac{|c_{02}|^2}{|c_{01}|^4} \quad (20)$$

Here we resort to the fact that $c_{00} \gg c_{10}, c_{10} \gg c_{20}, c_{02}, c_{11}$. Interestingly the second cavity occupation n_2 vanishes under the condition

$$F_2 = -i \frac{\chi}{\tilde{\Delta}_1} \quad (21)$$

which holds for F_2 real provided that $\Delta_1 = 0$. This corresponds to the condition where the laser driving of cavity 2 interferes destructively with the input $i\chi c_{10}$ from cavity 1. We can now look more specifically at the conditions required for $g_2^{(2)}(0)$ to vanish namely when $c_{02} = 0$. In such a case we obtain e.g. an optimal value for the cavity

1 pump amplitude

$$F_1|_{\text{opt}} = i \frac{F_2 \tilde{\Delta} \tilde{U}_1 \pm \sqrt{-F_2^2 U_1 \tilde{U}_1 \tilde{\Delta} \tilde{\Delta}_2}}{(\tilde{\Delta} + U_1) \chi} \quad (22)$$

where we defined $\tilde{\Delta} = \tilde{\Delta}_1 + \tilde{\Delta}_2$, $\tilde{U}_1 = \tilde{\Delta}_1 + U_1$.

STRONG PUMP LIMIT

Analytical linearized approach

In the opposed limit of strong pump amplitude where the cavity fields are dominantly classical, it is convenient to resort to standard linearization techniques allowing to check the convergence of the master equation results. The operators are expanded as $\hat{a}_j = \alpha_j + \delta \hat{a}_j$ given $\alpha_j = \langle \hat{a}_j \rangle$ the classical fields amplitudes and $\delta \hat{a}_j$ the quantum fluctuations operators. Dropping terms of orders larger than 2 in $\delta \hat{a}_j$ in Eq.(1) we can derive a set of linearized quantum Langevin equations

$$i \dot{\hat{a}}_1 = \left[-\Delta_1 + 4U_1 |\alpha_1|^2 - i \frac{\kappa_1}{2} \right] \hat{a}_1 \quad (23)$$

$$+ 2U_1 \alpha_1^2 \hat{a}_1^\dagger + i \sqrt{\kappa_1} \hat{a}_1^{\text{in}}$$

$$i \dot{\hat{a}}_2 = \left[-\Delta_2 + 4U_2 |\alpha_2|^2 - i \frac{\kappa_2}{2} \right] \hat{a}_2 \quad (24)$$

$$+ 2U_2 \alpha_2^2 \hat{a}_2^\dagger + i \sqrt{\kappa_2} \tilde{a}_2^{\text{in}}$$

for the fluctuations where we have dropped the δ notation. The operators \hat{a}_1^{in} and \tilde{a}_2^{in} account for the input noise in each cavities Here the cavity 1 output $\hat{a}_1^{\text{out}} = \sqrt{\kappa_1} \hat{a}_1 + \hat{a}_1^{\text{in}}$ is driving the cavity 2 input $\tilde{a}_2^{\text{in}} = \sqrt{\eta} \hat{a}_1^{\text{out}} + \sqrt{(1-\eta)} \hat{a}_2^{\text{in}}$ when an undelayed coupling is assumed and where \hat{a}_2^{in} is the local noise acting on cavity 2. The parameter $\eta \in [0, 1]$ stands for the fraction of cavity 1 field that is transmitted to the cavity 2. Hence we obtain

$$i \dot{\hat{a}}_1 = \left[-\Delta_1 + 4U_1 |\alpha_1|^2 - i \frac{\kappa_1}{2} \right] \hat{a}_1 \quad (25)$$

$$+ 2U_1 \alpha_1^2 \hat{a}_1^\dagger + i \sqrt{\kappa_1} \hat{a}_1^{\text{in}}$$

$$i \dot{\hat{a}}_2 = \left[-\Delta_2 + 4U_2 |\alpha_2|^2 - i \frac{\kappa_2}{2} \right] \hat{a}_2 \quad (26)$$

$$+ 2U_2 \alpha_2^2 \hat{a}_2^\dagger + i \sqrt{\eta \kappa_1 \kappa_2} \hat{a}_1$$

$$+ i \sqrt{\eta \kappa_2} \hat{a}_1^{\text{in}} + i \sqrt{(1-\eta) \kappa_2} \hat{a}_2^{\text{in}}$$

which reveal squeezing terms of strength $U_j \alpha_j^2$ governed by the steady state classical fields that fulfill

$$0 = \left[-\Delta_1 + 2U_1 |\alpha_1|^2 - i \frac{\kappa_1}{2} \right] \alpha_1 + F_1 \quad (27)$$

$$0 = \left[-\Delta_2 + 2U_2 |\alpha_2|^2 - i \frac{\kappa_2}{2} \right] \alpha_2 + F_2 - i \chi \alpha_1 \quad (28)$$

Eqs.(27,28) admit cumbersome but analytical solutions that can be plugged into Eq.(25,26) which can be recast

in the form $\dot{\mathbf{u}} = \hat{A} \mathbf{u} + \mathbf{n}$ where

$$\mathbf{u} = (\hat{a}_1, \hat{a}_1^\dagger, \hat{a}_2, \hat{a}_2^\dagger)^T \quad (29)$$

$$\mathbf{n} = (\sqrt{\kappa_1} \hat{a}_1^{\text{in}}, \sqrt{\kappa_1} \hat{a}_1^{\dagger \text{in}}, \sqrt{\eta \kappa_2} \hat{a}_1^{\text{in}} + \sqrt{(1-\eta) \kappa_2} \hat{a}_2^{\text{in}}, \sqrt{\eta \kappa_2} \hat{a}_1^{\dagger \text{in}} + \sqrt{(1-\eta) \kappa_2} \hat{a}_2^{\dagger \text{in}})^T \quad (30)$$

and

$$\hat{A} = -i \begin{pmatrix} \tilde{\Delta}_1 & 2U_1 \alpha_1^2 & 0 & 0 \\ -2U_1 \alpha_1^{2*} & -\tilde{\Delta}_1^* & 0 & 0 \\ -i\chi & 0 & \tilde{\Delta}_2 & 2U_2 \alpha_2^2 \\ 0 & i\chi & -2U_2 \alpha_2^{2*} & -\tilde{\Delta}_2^* \end{pmatrix} \quad (31)$$

where we used the definition $\tilde{\Delta}_j = -\Delta_j + 4U_j |\alpha_j|^2 - i \kappa_j / 2$. We can finally write the following Lyapunov equation

$$\hat{A} \hat{V} + \hat{V} \hat{A}^T = -\hat{D} \quad (32)$$

for the steady state correlation matrix

$$\hat{V} = \begin{pmatrix} \langle \hat{a}_1 \hat{a}_1 \rangle & \langle \hat{a}_1 \hat{a}_1^\dagger \rangle & \langle \hat{a}_1 \hat{a}_2 \rangle & \langle \hat{a}_1 \hat{a}_2^\dagger \rangle \\ \langle \hat{a}_1^\dagger \hat{a}_1 \rangle & \langle \hat{a}_1^\dagger \hat{a}_1^\dagger \rangle & \langle \hat{a}_1^\dagger \hat{a}_2 \rangle & \langle \hat{a}_1^\dagger \hat{a}_2^\dagger \rangle \\ \langle \hat{a}_2 \hat{a}_1 \rangle & \langle \hat{a}_2 \hat{a}_1^\dagger \rangle & \langle \hat{a}_2 \hat{a}_2 \rangle & \langle \hat{a}_2 \hat{a}_2^\dagger \rangle \\ \langle \hat{a}_2^\dagger \hat{a}_1 \rangle & \langle \hat{a}_2^\dagger \hat{a}_1^\dagger \rangle & \langle \hat{a}_2^\dagger \hat{a}_2 \rangle & \langle \hat{a}_2^\dagger \hat{a}_2^\dagger \rangle \end{pmatrix} \quad (33)$$

Given that in the absence of thermal photons the only non-zero noise correlations are $\langle \hat{a}_j^{\text{in}} \hat{a}_j^{\dagger \text{in}} \rangle$ the corresponding matrix reads

$$\hat{D} = \frac{1}{2} \begin{pmatrix} 0 & \kappa_1 & 0 & \chi \\ 0 & 0 & 0 & 0 \\ 0 & \chi & 0 & (1-\eta) \kappa_2 \\ 0 & 0 & 0 & 0 \end{pmatrix} \quad (34)$$

Eq.(32) can be vectorized in the form

$$\left(\hat{\mathbb{I}} \otimes \hat{A} + \hat{A} \otimes \hat{\mathbb{I}} \right) \text{vec}(\hat{V}) = -\text{vec}(\hat{D}) \quad (35)$$

which is nothing but a set of linear equation solvable analytically. Then, from the knowledge of \hat{V} , we can compute the second order coherence functions as

$$g_j^{(2)}(0) \simeq \frac{N_j^2 + 4n_j N_j + 2n_j + 2 \text{Re} [\alpha_j^{*2} \langle \hat{a}_j^2 \rangle] + |\langle \hat{a}_j^2 \rangle|^2}{[n_j + N_j]^2} \quad (36)$$

with the definitions $N_j = |\alpha_j|^2$ and $n_j = \langle \hat{a}_j^\dagger \hat{a}_j \rangle$ for the classical and fluctuation populations respectively. Finally we note that while such linearized approach only allows for gaussian states, it remains suitable for the description of squeezed states.

Semiclassical Approach

While the above linearized approach allows to efficiently compute the steady state solutions and is especially suitable for optimization, it cannot directly address

the system dynamics, disregards non-Gaussian states and doesn't give access to the system density matrix. If needed one can therefore deploy a semiclassical approach to overcome these limitations where the classical field dynamics is governed by

$$i\dot{\alpha}_1 = \tilde{\Delta}_1\alpha_1 + F_1(t) \quad (37)$$

$$i\dot{\alpha}_2 = \tilde{\Delta}_2\alpha_2 + F_2(t) - i\chi\alpha_1 \quad (38)$$

and the fluctuations are evolving according to the master equation

$$i\frac{\partial \hat{\rho}_f}{\partial t} = [\hat{\mathcal{H}}_f, \hat{\rho}_f] - \frac{i}{2} \sum_{j=1,2} \kappa_j \hat{\mathcal{D}}[\delta \hat{a}_j] \hat{\rho}_f + i\chi \hat{\mathcal{D}}[\delta \hat{a}_1, \delta \hat{a}_2] \hat{\rho}_f \quad (39)$$

where the associated Hamiltonian reads

$$\begin{aligned} \hat{\mathcal{H}}_f = & \sum_{j=1,2} \left[\tilde{\Delta}_j \hat{a}_j^\dagger \hat{a}_j + U_j \left(\alpha_j^* \hat{a}_j^2 + \alpha_j^2 \hat{a}_j^{\dagger 2} \right) \right] \\ & + \sum_{j=1,2} U_j \left[\hat{a}_j^\dagger \hat{a}_j^\dagger \hat{a}_j \hat{a}_j + 2\alpha_j^* \hat{a}_j^\dagger \hat{a}_j \hat{a}_j + 2\alpha_j \hat{a}_j^\dagger \hat{a}_j^\dagger \hat{a}_j \right] \end{aligned} \quad (40)$$

dropping the δ notations. Note that we keep here non-linear terms of all orders for an exact description of the system. The advantage of this method with respect to the direct master equation treatment stems from the fact that the fluctuation occupation is very small in the displaced reference frame set by the classical field which allows to work with a much smaller truncated Hilbert space and this at an arbitrary pump power. It turns into a great advantage for the global optimization routine that converges much faster and small memory cost in the semiclassical case. If needed, the full system density matrix can be reconstructed applying a multimode displacement operator according to

$$\hat{\mathcal{D}}(\alpha_1, \alpha_2) = e^{\alpha_1 \hat{a}_1^\dagger - \alpha_1^* \hat{a}_1} e^{\alpha_2 \hat{a}_2^\dagger - \alpha_2^* \hat{a}_2} \quad (41)$$

$$\hat{\rho} = \hat{\mathcal{D}}(\alpha_1, \alpha_2) \hat{\rho}_f \hat{\mathcal{D}}^\dagger(\alpha_1, \alpha_2) \quad (42)$$

where $\hat{\rho}_f$ as been preliminary inflated with zeros to a suitable size imposed by the classical amplitudes. Any correlation can be accessed by reconstructing the global operators $\hat{a}_j(t) = \alpha_j(t)\mathbb{I} + \delta \hat{a}_j$ evaluated on $\hat{\rho}_f(t)$.

OPTIMAL PULSE DELAY

As discussed in the main text, the $g_{\text{pulse}}^{(2)}$ can be minimized by imposing the proper delay $\Delta t = t_{02} - t_{01}$ between the cavity pulses. We have therefore computed in Fig.S2 the $g_{\text{pulse}}^{(2)}$ dependance versus Δt for the parameters of Fig.5 which demonstrates the occurrence of an optimal value.

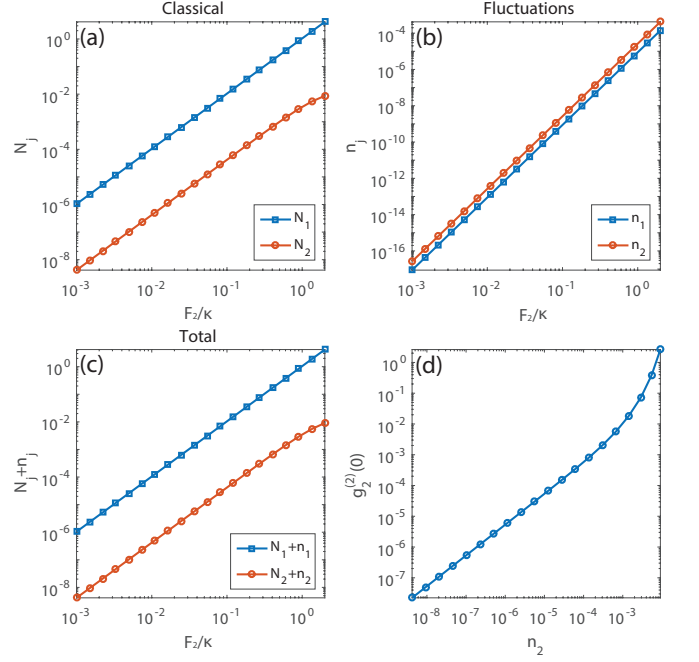


Fig.S 1: (Color online) Semiclassical steady state solutions for the parameters of Fig.2 of the main text under the optimal condition. (a) Classical, (b) fluctuations and (c) total cavity occupations versus the pump amplitude F_2 . (d) Cavity 2 second order coherence function versus its occupation $n_2 + N_2$.

UNIDIRECTIONAL COUPLING

In the main text we proposed the three cavity configuration as a candidate system for the required dissipative coupling. The corresponding Hamiltonian reads

$$\begin{aligned} \hat{\mathcal{H}} = & \sum_{j=1}^3 \left[-\Delta_j \hat{a}_j^\dagger \hat{a}_j + U_j \hat{a}_j^\dagger \hat{a}_j^\dagger \hat{a}_j \hat{a}_j + F_j^* \hat{a}_j + F_j \hat{a}_j^\dagger \right] \\ & + \sum_{j \neq k=1}^3 \left[J_{jk} \hat{a}_j^\dagger \hat{a}_k + J_{jk}^* \hat{a}_k^\dagger \hat{a}_j \right] \end{aligned} \quad (43)$$

and the master equation takes the standard form

$$i\frac{\partial \hat{\rho}}{\partial t} = [\hat{\mathcal{H}}, \hat{\rho}] - \frac{i}{2} \sum_{j=1}^3 \kappa_j \hat{\mathcal{D}}[\hat{a}_j] \hat{\rho} \quad (44)$$

We set the conditions $J_{12} = i\chi/2$, $J_{23} = J_{31} = \sqrt{-iJ_{12}\kappa_3/2}$, $F_3 = 0$, $U_1 = U_2 = U_3 = 1e - 3\kappa$, $\kappa_1 = \kappa_2 = \kappa$ and $\kappa_3 = 10\kappa$. To demonstrate the unidirectional transmission we solve the system dynamics through Eq.(44), in the cases where only one cavity is driven as shown in Fig.S3 and setting the nonzero pump amplitude to 0.1κ . As one can see, while driving the cavity 1 solely results in a nonzero field in the cavity 2, driving only the latter results in a vanishing cavity 1 occupation as expected. It demonstrates the efficient

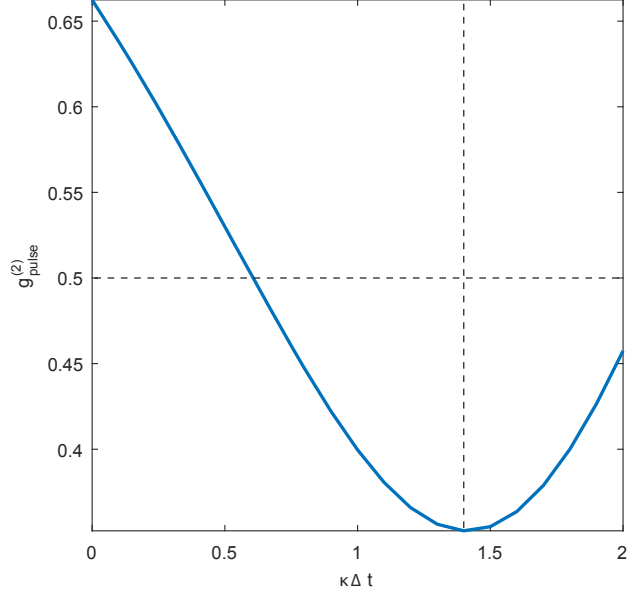


Fig.S 2: (Color online) Integrated cavity 2 emission statistics $g_{\text{pulse}}^{(2)}$ at variable delays Δt between the pulses.

unidirectional transmission from cavity 1 to cavity 2 in the parameter range we consider.

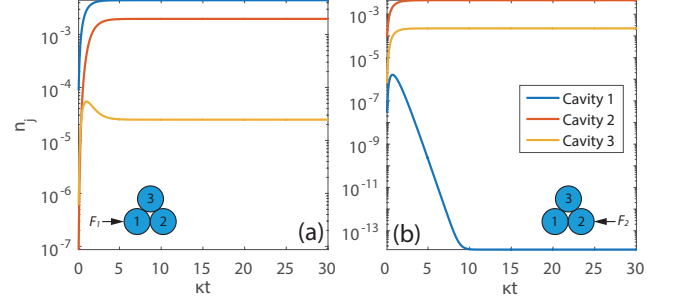


Fig.S 3: (Color online) Log scale cavity occupations in the case where we drive (a) only the cavity 1: $F_1 = 0.1\kappa$ and $F_2 = 0$ (b) only the cavity 2: $F_1 = 0$ and $F_2 = 0.1\kappa$. The parameters are those of Tab.II of the main text.